A Multi-Stage Optimization Approach for Active Distribution Network Scheduling Considering Coordinated Electrical Vehicle Charging Strategy

XIAOJUN ZHU[1], HAITENG HAN[2], (Student Member, IEEE), SHAN GAO[2], (Member, IEEE), QINGXIN SHI[3], (Student Member, IEEE), HANTAO CUI[3], (Student Member, IEEE), AND GUOQIANG ZU[4], (Student Member, IEEE)

[1]State Grid Jiangsu Economic Research Institute, Nanjing 210008, China
[2]School of Electrical Engineering, Southeast University, Nanjing 210096, China
[3]Center for Ultra-wide-area Resilient Electric Energy Transmission Networks, Department of Electrical Engineering and Computer Science, The University of Tennessee, Knoxville, TN 37996, USA
[4]State Grid Tianjin Electric Power Company Electric Power Research Institute, Tianjin 300022, China

Corresponding author: Haiteng Han (hanhtseu@gmail.com)

ABSTRACT The increasing integration of renewable resources and electric vehicles (EVs) presents new requirements for the construction of a current distribution network. As an alternative of conventional distribution network, active distribution network (ADN) has gained more interest for its flexibility and interactivity. However, the unpredictable behavior of ADN participants from source-side, network-side, and demand-side brings more challenges on ADN dispatch. Thus, it is urged to design an ADN optimal scheduling approach that can comprehensively regulate the ADN participants' behavior. In this paper, an ADN performance assessment system is first established to provide a quantitative analysis on ADN's scheduling in terms of active controllability, active manageability, and active economy, respectively. Then, according to the ADN assessment system, a multi-stage optimal scheduling approach for ADN considering coordinated EV charging strategy is proposed. It is able to not only smooth the fluctuations caused by the integration of intermittent power sources and EVs but also reconfigure the network topology. Therefore, this approach can be applied to day-ahead dispatches to help operators effectively manage the ADN. Simulation results verify the correctness and effectiveness of the proposed approach.

INDEX TERMS Active distribution network scheduling, electric vehicle, coordinated charging strategy, distributed energy resource.

NOMENCLATURE
The mathematical symbols of this paper are classified as follows:

A. SETS
ψ Set of EVs in the specific region.
Ω Set of starting time of charging with the lowest charging price.
A_t Set of unavailable charging stations at time t.
B_t Set of available charging stations at time t.

B. VARIABLES
$U(t)\%$ Qualified voltage ratio at time t.
N_{V-over} The number of buses with overvoltage.
$N_{V-under}$ The number of buses with undervoltage.
$L(t)$ Primary line load ratio at time t.
$P_{pri}(t)$ The active power transmitted through primary lines at time t, (kW).
P_{pri}^{max} The maximum active power transmitted through primary lines, (kW).
C_{avg} Average charging cost of EVs in the specific region, (CNY).

C_j — Charging cost of the jth EV, (CNY).

$E_{full}\%$ — EV fully-charged ratio in the typical day.

N_{t_full} — The number of fully-charged EVs.

$D_0(t)$ — The traditional load at time t, (kW).

$D_e(t)$ — The equivalent load at time t, (kW).

$\bar{D}_e$ — The mean value of equivalent load, (kW).

$\Pi_{IL}(t)$ — Total cost of the interruptible load compensation at time t, (CNY).

$P_{IL,i}(t)$ — Active power of interruptible load on bus i at time t, (kW).

$\Pi_{loss}(t)$ — Total distribution system loss cost at time t, (CNY).

$P_{loss}(t)$ — Distribution system loss at time t, (kW).

$P_W(t)$ — Output of wind power at time t, (kW).

$P_{PV}(t)$ — Output of solar power at time t, (kW).

$P_{EV}(t)$ — EV charging power at time t, (kW).

$P_{MT}(t)$ — Output of microturbine at time t, (kW).

$P_0(t)$ — Purchased electricity from transmission grid at time t, (kW).

$S_i(t)$ — The status of ith switch at time t ($S_i(t) = 0$, switch off and $S_i(t) = 1$, switch on).

$l(t)$ — The overload level of primary line at time t.

P_i — Injected active power to bus i, (kW).

Q_i — Injected reactive power to bus i, (kVar).

θ_{ij} — Phase angle difference between bus i and bus j.

U_i — Voltage amplitude of bus i, (kV).

$P_{shed}(t)$ — Shedding load at time t, (kW).

$P_i(t)$ — The load on bus i at time t, (kW).

C. CONSTANTS

N_{all} — The number of total buses.

N_ψ — The number of total EVs.

π_{switch} — The price of switch operation, (CNY).

π_i — The compensation price of interruptible load on bus i, (CNY/kW · h).

π_{loss} — The price of distribution system loss, (CNY/kW · h).

π_W — The price of wind power integration, (CNY/kW · h).

π_{PV} — The price of solar power integration, (CNY/kW · h).

π_{MT} — The price of microturbine integration, (CNY/kW · h).

π_0 — The price of electricity purchased from the transmission grid, (CNY/kW · h).

π^{CO_2} — Penalty factor of CO_2 emission, (CNY/g).

π^{SO_2} — Penalty factor of SO_2 emission, (CNY/g).

$Q_{MT}^{CO_2}$ — CO_2 emission quantity of microturbine, (g/kW · h).

$Q_{MT}^{SO_2}$ — SO_2 emission quantity of microturbine, (g/kW · h).

$Q_0^{CO_2}$ — CO_2 emission quantity of traditional power plant, (g/kW · h).

$Q_0^{SO_2}$ — SO_2 emission quantity of traditional power plant, (g/kW · h).

P_{ch} — Charging power of EV, (kW).

ω_1 — Weighting coefficient associated with the switch operation cost.

ω_2 — Weighting coefficient associated with the distribution system loss cost.

ω_3 — Weighting coefficient associated with the power source integration cost.

ω_4 — Weighting coefficient associated with the environmental pollution penalty.

p_1 — Penalty factor associated with unqualified voltage ratio.

p_2 — Penalty factor associated with primary line load ratio.

L_0 — The maximum primary line load ratio.

G_{ij} — Real part of each element in the admittance matrix.

B_{ij} — Imaginary part of each element in the admittance matrix.

U_i^{min}/U_i^{max} — Lower/upper voltage amplitude limit of bus i, (kV).

S_j^{max} — Maximum transmission capacity of line j, (kVA).

$P_{MT,i}^{min}/P_{MT,i}^{max}$ — Lower/upper output of i th microturbine, (kW).

p_{shed} — The compensation price of load shedding, (CNY/ kW · h).

$\eta\%$ — The load shedding coefficient required by the contract.

I. INTRODUCTION

Concerns on energy policies and environmental conditions lead to a rapid development of renewable energy resources, such as wind turbine and solar systems, being integrated into power systems in a global scale [1], [2]. The increasing penetration of these distributed energy resources (DERs) challenges the power system stability and security. It also imposes requirements on the traditional distribution networks [3]. To address this issue, the active distribution network has attracted more attention in recent years because it is capable of actively managing and controlling the DERs and loads by utilizing a smart network topology.

In practice, the load scheduling is the key point to distribution network studies. The advancement of communication and automation technology paves the way for the development of ADN, which is developing into a multi-dimensional system consisting of participants from source-side, network-side, and demand-side. With more dispatchable participants such as DERs and interruptible-load in the multi-dimensional system, the optimal scheduling of ADN experiences different process from that of the traditional distribution networks [4].

Meanwhile, the electric vehicle is being introduced into the distribution networks [5]. EV can participate in ADN's demand-side scheduling due to the dispatchable characteristics in the charging process [6], [7]. However, it should be noted that the uncertainties in EV charging behavior is unavoidable. In other words, without any appropriate

guidance and management, the integration of EV probably widens the gap between the peak and valley load in the regional ADN, deteriorating the power quality during the peak-load time.

Hence, it is of great importance to regulate the EV's charging mode in the ADN environment, and form an appropriate ADN optimal scheduling approach that can comprehensively consider the behavior of participants from source-side, network-side, and demand-side. Nevertheless, current research on these issues is rarely done. Most of the traditional works are focused on the individual behavior of the ADN participants. Reference [8] provides a distribution network scheduling framework including wind power and solar energy based on the complementary features of DERs. By complementing a coordinated control strategy on the wind power and photovoltaic (PV) outputs, the fluctuations of these intermittent resources are notably relieved. In [9], wind/PV hybrid power fluctuations are reduced via the optimization of the energy storage capacity. However, these approaches are focused on the source-side scheduling. Examples of network-side behavior are studied in [10]–[14]. References [10]–[12] aim at utilizing artificial intelligence algorithms to implement the network reconfiguration and improving the comprehensive benefits of the distribution networks. References [13], [14] consider the impacts of fault restoration on the network reconfiguration. Furthermore, extensive research has been conducted from the perspective of demand-side activities [15]–[18]. Reference [19] proposes an effective load scheduling method based on a time-of-use (TOU) price model. In addition, as a significant participant in the ADN's demand-side, EV behavior has a notable impact on ADN's operation. Reference [20] shows that the integration of a large number of random EV charging loads can obviously affect the power quality. It presents a quantitative approach to analyze the increased distribution system loss due to EVs' unregulated behavior. By contrast, a coordinated EV charging strategy is quite helpful in improving load condition of transmission lines [21]. Furthermore, [22] and [23] illustrate that the EV's behavior can be regulated by energy management strategies, which contributes to the fuel consumption reduction and the stability of distribution networks. Besides, research works in which EV dispatch incorporates with renewable resources can be seen in [24]–[26]. An optimal integration approach of a hybrid solar battery power source into smart home grid with EV is proposed in [24], which significantly reduces the customers' electric cost. Reference [25] analyzes the impacts of EV charging behavior on load-fluctuation control based on an incorporated scheduling model including EV and wind power. Reference [26] verifies the promoting function of EV charging control in wind power consuming and greenhouse gas emission limiting.

To enhance the security, economic and environmental benefits of ADN under the incorporated source-network-load condition, we focus on the ADN optimal scheduling approach through regulating the behavior of ADN participants from source-side, network-side, and demand-side in this paper. The contributions include: 1) A quantitative assessment system on ADN performance is proposed, according to the characteristics of ADN. 2) A coordinated EV charging strategy is established. Then, a multi-stage ADN optimization consisting of controllable distributed generator (DG), network topology, and interruptible load is considered.

The rest of the paper is organized as follows. Section II establishes an assessment system for ADN considering active controllability, active manageability, and active economy. Section III provides a coordinated EV charging approach, and then models a multi-stage optimal scheduling strategy. Section IV verifies the effectiveness of the proposed strategy with simulations. Finally, Section V draws conclusions for the presented studies and provides directions for future research.

II. ASSESSMENT SYSTEM FOR ADN PERFORMANCE

In this section, we model the ADN performance assessment system in which the characteristics of ADN in three aspects (active controllability, active manageability, and active economy) are integrated. Accordingly, multiple indices reflecting the security, economic, and environmental cost in the power system operation are proposed.

A. ACTIVE CONTROLLABILITY

Active controllability reflects the impacts of power system dispatch scheme on ADN stability and security, which can be represented by qualified voltage ratio, primary line load ratio, and reconfiguring switch frequency. These indices are related to distribution feeders.

1) QUALIFIED VOLTAGE RATIO

Qualified voltage ratio is the percentage of the qualified voltage bus amount in total buses, reflecting the controllable effectiveness. It is expressed as:

$$U(t)\% = 1 - \frac{N_{V-over} + N_{V-under}}{N_{all}} \times 100\% \qquad (1)$$

2) PRIMARY LINE LOAD RATIO

Primary line load ratio, expressed in (2), reflects the margin level of transmission line capacity in a regional power grid, which can be utilized to verify the extensibility of regional grid. Note that a larger value of the index indicates that the regional grid cannot probably satisfy the future load demand.

$$L(t) = \frac{P_{pri}(t)}{P_{pri}^{\max}} \times 100\% \qquad (2)$$

3) RECONFIGURING SWITCH FREQUENCY

The reconfiguring process in ADN optimization aims at reducing distribution system loss, enhancing load balance level, and improving the economy of power grid operation. Thus, reconfiguring switch frequency is taken account into this process as a significant index. It is inadvisable to be much high in terms of requirements on switch service life and

power system stability. Also, the switch operation cost can be expressed as:

$$\Pi_{switch}(t) = \pi_{switch} \times \sum_{i=1}^{N_s} |S_i(t) - S_i(t-1)| \tag{3}$$

B. ACTIVE MANAGEABILITY

Active manageability mainly reflects the contribution of demand-side optimal approaches in ADN scheduling. In this paper, we focus on the coordinated EV charging guidance and load shedding. Therefore, we establish three indices including EV customer satisfaction level, equivalent load curve standard deviation, and interruptible load compensation. These indices are related to distribution system load.

1) EV CUSTOMER SATISFACTION LEVEL

Actually, the EV charging strategy is bidirectional since it is related to not only the electricity companies' benefits but also the EV customers' benefits. From the perspective of EV customers, the charging cost and charging capacity are the most important factors. Thus, the two factors are taken account into the EV customer satisfaction level indices.

With the help of EV scheduling system, the customers are more inclined to adjust their charging time to reduce the charging cost. Here, for consideration of all the customers' satisfaction levels in a specific regional grid, the average charging cost of EVs is chosen as one of the EV customer satisfaction level indices, which can be expressed as:

$$C_{avg} = \frac{\sum_{j \in \psi} C_j}{N_\psi} \tag{4}$$

In addition, the charging schemes can change the charging capacity of each electrical vehicle, and then impact the customer satisfaction level, i.e. if an electrical vehicle is not fully charged during the parking period, the satisfaction level of its owner will be definitely reduced. Thus, we use EV fully-charged ratio in (5) to represent the charging capacity factor in customer satisfaction level indices. Note that the battery capacity of each EV is assumed to be the same.

$$E_{full}\% = \left(\sum_{t=1}^{n} \frac{N_{t\_full}}{N_\psi} \right) \times 100\% \tag{5}$$

2) EQUIVALENT LOAD CURVE STANDARD DEVIATION

When EVs are integrated into the grid without any coordinated charging strategy, a new peak load probably overlays on the peak point of the initial load curve, which can widen the gap between the peak and valley load. By contrast, with the help of a coordinated management of EV charging mode, the peak shaving and valley filling functions can be better implemented. To quantify the effectiveness of active manageability in the integral ADN load curve, we first define the equivalent load in (6), and then establish the equivalent load

curve standard deviation index in (7).

$$D_e(t) = D_0(t) - P_W(t) - P_{PV}(t) + P_{EV}(t) \tag{6}$$

$$\begin{cases} \bar{D}_e = \dfrac{1}{T} \sum_{t=1}^{T} D_e(t) \\[3mm] S_e = \sqrt{\dfrac{1}{T} \sum_{t=1}^{T} \left(D_e(t) - \bar{D}_e \right)^2} \end{cases} \tag{7}$$

3) INTERRUPTIBLE LOAD COMPENSATION

Generally, after signing a contract with customers, the electricity company is allowed to interrupt the normal load when system overload occurs. Also, the electricity company is supposed to provide compensation to customers at a contract price. The interruptible load compensation index can be expressed as:

$$\Pi_{IL}(t) = \sum_i \pi_i \times P_{IL,i}(t) \tag{8}$$

C. ACTIVE ECONOMY

The operation economy is always a key index in power system optimal scheduling. With the enhancing awareness of environmental protection, the environmental benefit is also brought into the power grid, especially the ADN economic dispatch. Thus, we establish the active economy indices in three aspects, including distribution system loss cost, power source integration cost, and environmental pollution penalty.

1) DISTRIBUTION SYSTEM LOSS COST

Distribution system loss cost reflects not only the reasonability of grid structure but also the economy of grid operation. With a lower distribution system loss cost, the electricity company can gain more profits.

$$\Pi_{loss}(t) = \pi_{loss} \times P_{loss}(t) \tag{9}$$

2) POWER SOURCE INTEGRATION COST

In this paper, the index includes in part of wind power, PV, and microturbine integration cost and in part of the purchased electricity cost.

$$\Pi_{source}(t) = \pi_W P_W(t) + \pi_{PV} P_{PV}(t) + \pi_{MT} P_{MT}(t) + \pi_0 P_0(t) \tag{10}$$

3) ENVIRONMENTAL POLLUTION PENALTY

The environmental impact is converted to the economy index in the ADN scheduling model. In addition, we choose CO_2 and SO_2 as two typical pollutants to establish the environmental pollution penalty index.

$$\Pi_{penalty}(t) = \pi^{CO_2} \sum \left(P_{MT}(t) Q_{MT}^{CO_2} + P_0(t) Q_0^{CO_2} \right)$$
$$+ \pi^{SO_2} \sum \left(P_{MT}(t) Q_{MT}^{SO_2} + P_0(t) Q_0^{SO_2} \right) \tag{11}$$
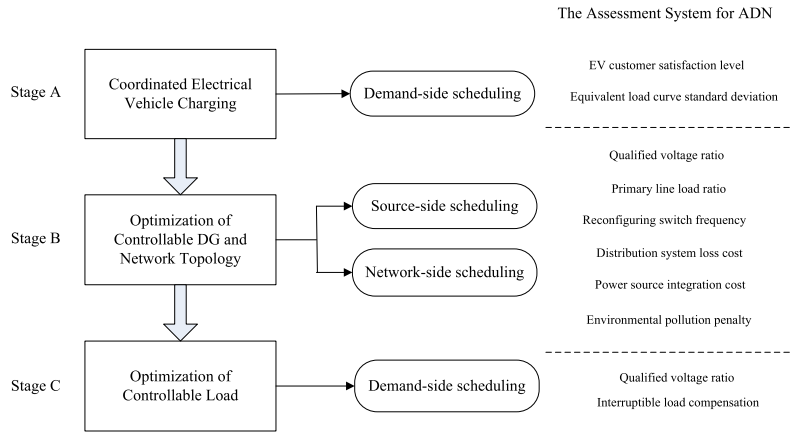
FIGURE 1. Overview of the multi-stage ADN optimal scheduling strategy.

III. MULTI-STAGE OPTIMIZATION MODEL FOR ADN SCHEDULING

The ADN optimal scheduling experiences three stages considering all the resources in source-side, network-side, and demand-side. The overview of the scheduling process is presented in Fig. 1 and the scheduling in each stage is based on the aforementioned indices in Section II.

A. STAGE A: COORDINATED ELECTRICAL VEHICLE CHARGING

The coordinated EV charging scheduling aims at improving the conventional EV charging mode. It is established according to EV's driving and charging characteristics. Also, the EV charging time, location, and scheme are all considered in the coordinated EV charging model.

1) CONVENTIONAL EV CHARGING MODEL

The main purpose of the EV charging model is to obtain the charging load when EVs in a specific scale are integrated into the grid. The conventional approaches can be classified into three categories: deterministic demand-based method [27], Monte Carlo simulation (MCS) method [28], and probabilistic charging-station-load–based analytical method [29]. MCS is utilized in this paper since it has the highest precision among the three methods. The total charging load can be calculated according to the MCS data which contains each EV's driving status, charging time, charging location, and charging scheme within a typical day.

2) COORDINATED EV CHARGING MODEL

With the advancement of communication technology, the EV charging scheduling system can provide a favorable support platform for the coordinated EV charging strategy. Fig. 2 shows a typical EV charging scheduling system.

Customers prefer the EV charging scheduling system that can respond to the peak-and-valley electricity price. In addition, EV charging locations are optimized under the guidance of a coordinated scheduling strategy. It can not only enhance the charging efficiency but also improve the
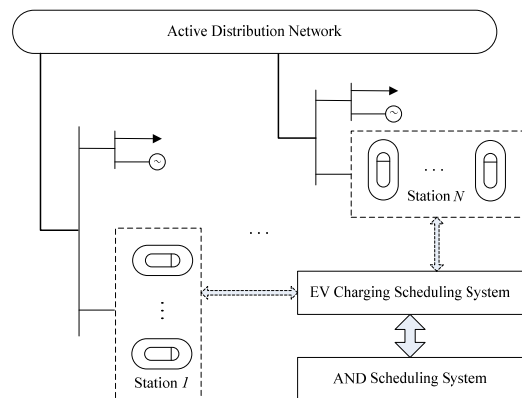

FIGURE 2. The typical EV charging scheduling system.

EV customers' satisfaction level. Thus, we establish the coordinated EV charging scheduling model considering charging time, charging location, and charging scheme.

① *Optimization of Charging Time:* In the conventional EV charging process, the customers charge their EVs as soon as they arrive at the charging location. By contrast, in the coordinated EV charging process, customers can input the arrival time, departure time, and the expected charging capacity. Then, the EV charging scheduling system will provide a coordinated charging strategy based on the peak-and-valley electricity price.

Assume that an EV's arrival time and expected departure time are t_{arr} and t_{dep}, respectively. The corresponding battery capacities are W_1 and W_2, respectively. Thus, the expected parking time T_p can be expressed as:

$$T_p = t_{dep} - t_{arr} \qquad (12)$$

The expected charging capacity W_{ch} is:

$$W_{ch} = W_2 - W_1 \qquad (13)$$

Then, the fully-charged required time T_r is:

$$T_r = \frac{W_{ch}}{P_{ch}} \qquad (14)$$

During the parking period, the EV charging scheduling system is to ensure that the customers obtain the earliest charging service at the lowest cost, which not only reduces the gap between the peak and valley equivalent load, but also improves the EV customers' satisfaction level. The actual starting time of charging t_{ch} and the charging cost p are expressed as (15) and (16), respectively.

$$t_{ch} = \begin{cases} t_{arr}, & T_r \geq T_p \\ \min \Omega, & T_r \leq T_p \end{cases} \quad (15)$$

$$p = \min \sum_{t_s}^{t_s + t_{dep} - t_{ch}} (P_{ch} \pi_t^{EV}) \Delta t, \quad t_s \in \Omega \quad (16)$$

where π_t^{EV} is the EV charging price at time t, t_s is the simulated starting time of charging, and t is the interval time which is equal to 1 h.

② *Optimization of Charging Location:* In the conventional EV charging mode, customers have to wait for the next charging chance when the current charging station is completely occupied. By contrast, with a coordinated EV charging scheduling strategy considering the optimization of charging location, the EV customers can be guided to the nearest available charging station.

$$q = \begin{cases} (j|j \in B_t), & i \in A_t \\ i, & i \in B_t \end{cases} \quad (17)$$

where q is the charging location ID at time t provided by the coordinated EV charging scheduling strategy.

③ *Optimization of Charging Scheme:* Although the slow charging scheme is friendly to EV battery, it is a time-consuming process which generally requires 6-8 hours to fully charge the EVs [30]–[32]. In addition, it is harder for the charging stations to serve the coming EV customers when most slow charging piles are occupied. In recent years, more charging stations have assembled fast charging piles with the advancement of charging technology, which complementally supports the charging service for the increasing EV customers' demand. However, compared with the slow charging scheme, the EV battery life will be harmed by the fast charging scheme.

Thus, in this paper we design a comprehensive charging mode in which the fast charging scheme is considered as a complementary approach for the dominant slow charging scheme. The following assumptions are made:

- The EV customers are inclined to choose the fast charging scheme when they arrive early at the stations nearby office zone during the day time.
- Customers choose the slow charging scheme when they park their EVs at the stations nearby residence zone during the night time.

3) DISCUSSIONS ON MODELS AND ASSUMPTIONS
To model the EV charging behavior in the ADN environment, we adopt simplified component models and make corresponding assumptions.

For the uncertainties of the EV charging model, we focus on the temporal uncertainties and model it in statistical terms. Four probabilistic parameters regarding EV's charging time are selected. Also, we assume that each parameter follows a typical Gaussian distribution listed in Appendix. The EV charging status is then obtained by Monte Carlo simulation sampling. For spatial uncertainties [35], this paper does not explore too much due to the complexity of model as the uncertain spatial effects are considered.

In addition, the EV battery degradation [36], [37] is not considered. Since this paper is focused on optimizing the EV charging behavior in a G2V implementation scenario, obtaining the EV load demand has higher priority.

Thus, with the consideration of model complexity and computation efficiency, we simplify the EV charging model. However, these two concerns are definitely significant extensions for this work.

B. STAGE B: OPTIMIZATION OF CONTROLLABLE DG AND NETWORK TOPOLOGY
In Stage B, we synchronously optimize the controllable DG and network topology. Also, the optimal objectives consist of the economy benefit and the environmental benefit. The dual-objective problem is converted to a single-object problem by integrating weight coefficients.

The recast optimal objective in Stage B contains the main function represents economy and environmental objectives, and the penalty function representing security objective.

The main function:

$$\min M(t) = \omega_1 \times \Pi_{switch}(t) + \omega_2 \times \Pi_{loss}(t) + \omega_3 \\ \times \Pi_{source}(t) + \omega_4 \times \Pi_{penalty}(t) \quad (18)$$

where $\Pi_{switch}(t)$, $\Pi_{loss}(t)$, $\Pi_{source}(t)$, and $\Pi_{penalty}(t)$ can be obtained according to (3), (9), (10), and (11), respectively.

The penalty function:

$$P(t) = p_1 \times (1 - U(t)\%) + p_2 \times l(t)$$
$$l(t) = \begin{cases} 0, & L(t) \leq L_0 \\ L(t) - L_0, & L(t) \geq L_0 \end{cases} \quad (19)$$

where both p_1 and p_2 are big values.

Thus, the integrated optimal objective problem can be formulated as:

$$\min M(t) + P(t) \quad (20)$$

subject to:

$$\begin{cases} P_i = U_i \sum_{j=1}^{n} U_j (G_{ij} \cos \theta_{ij} + B_{ij} \sin \theta_{ij}) \\ Q_i = U_i \sum_{j=1}^{n} U_j (G_{ij} \sin \theta_{ij} - B_{ij} \cos \theta_{ij}) \end{cases} \quad (21)$$

$$U_i^{\min} \leq U_i \leq U_i^{\max} \quad (22)$$

$$S_j \leq S_j^{\max} \quad (23)$$

$$P_{G,i}^{\min} \leq P_{G,i} \leq P_{G,i}^{\max} \quad (24)$$

Constraint (21) represents the active and reactive power flow balancing. Note that the AC power flow model is selected in this paper and the backward-forward sweep method [33], [34] is utilized in the optimization process regarding the power flow computation. Also, the aforementioned distribution system loss is derived from the power flow results. Constraint (22) impose the upper and lower limits of the voltage amplitude on bus *i*. Constraint (23) requires that the power flow of each transmission line must be less than the rated value. Constraint (24) ensures that the outputs of microturbines are limited by their maximum and minimum outputs. In addition, the optimization process must satisfy the general distribution network constraints such as connectivity constraint and radial constraint.

C. STAGE C: OPTIMIZATION OF CONTROLLABLE LOAD

The optimization of controllable load is the last stage in the total ADN optimal scheduling strategy. It works after that both the aforementioned optimization approaches cannot appropriately deal with problems like low voltage and over-load in the system operation.

The optimal scheduling on this stage includes two parts: 1) EV load shedding; and 2) Interruptible load dispatch. In the first step, EV charging piles will shut down after receiving instruction from the EV charging scheduling system and keep the off-status until receiving a restart instruction.

If the grid voltage level cannot recover to the normal level with EV load shedding, then the interruptible load dispatch will be implemented. The objective function is formulated as:

$$\min \ p_{shed} \times P_{shed}(t) + p_1 \times (1 - U(t)\%) + p_2 \times l(t) \quad (25)$$

$$\text{subject to: constraints in } (21) - (23) \quad (26)$$

$$P_{shed,i}(t) \le P_i(t) \times \eta\% \quad (27)$$

Detailed process of the multi-stage optimization approach is illustrated in Fig. 3 and a genetic algorithm is utilized in the optimization.

IV. CASE STUDY

To demonstrate the effectiveness of the proposed approach, the verification study has been done with a modified IEEE 33-bus distribution system, as shown in Fig. 4. All simulations are based on MATLAB environment. The simulation period is set to 24 *h* time horizon and the interval time is set to 1 *h*.

Assume that the resident loads are assigned on bus 22, 23, 24, 28, 29, 30, 31, and 32, respectively, and the commercial loads on the other buses. Locations of the 20 EV charging stations are also shown in Fig. 4 and each station has 35 charging piles. The total amount of EVs is set to 500 and the battery capacity of each EV is 32 kW·h. The charging power is set to 3.2 kW in slow charging scheme and 15 kW in fast charging scheme. The time-of-use (TOU) price policy is implemented in this paper. It is designed according to the load fluctuations in the typical day, as shown in Appendix. In addition, two wind farms are connected to bus 17 and 21, respectively, and two PV stations are located on bus 24 and 32, respectively.

The outputs of the two intermittent sources and the load can be found in Appendix as well.

A. COORDINATED ELECTRICAL VEHICLE CHARGING SCHEDULING OPTIMIZATION

The charging status of the 20 EV charging stations in the typical day are simulated, and the impacts of charging time, charging location, and charging scheme in the coordinated EV charging scheduling process are compared, as shown in Fig. 5. The horizontal axis represents the time range of a typical day with the sampling frequency set to every 15 minutes, and the vertical axis represents the number of charging EVs (also the number of charging piles in use). Then, the curves with 20 different colors are obtained by connecting all the relevant number of charging EVs at each sampling time, which reflect the charging status of the 20 EV charging stations. Also, values of the EV fully-charged ratio in different charging modes are listed in TABLE 1. The conventional charging mode, coordinated charging mode with time optimization, coordinated charging mode with time and location optimization, and coordinated charging mode with time, location, and scheme optimization are represented by C0, C1, C2, and C3, respectively.

TABLE 1. Values of the EV Fully-charged ratio in different charging modes.

EV Charging Mode	Fully-charged ratio after departing from official zone	Fully-charged ratio after departing from resident zone
C0	65.20%	96.20%
C1	62.20%	80.00%
C2	65.20%	81.40%
C3	96.40%	99.00%

It can be observed that in C1, C2, and C3, the EV charging period becomes more dispersive. More EV customers receive the charging service around at 9 a.m. and 12~4 p.m. in the official zone, and 1~6 a.m. in the resident zone, which is quite different from that in C0. The shift of charging period significantly alleviates the EV charging congestion. Note that the EV charging congestion is even eliminated in C3, which reflects that the coordinated EV charging strategy can provide an economical guidance on the assembling quantity of charging piles.

In addition, the fully-charged ratio in C1 is less than that in C0. It is convincible that EV charging piles are occupied by the customers early arriving at charging stations. Also, in order to respond to a preferable charging price, the customers at the same charging station tend to start receiving charging service within a relative concentrated period, which further degrades the fully-charged ratio. To deal with this issue, the optimization of charging location and charging scheme is added to the coordinated scheduling strategy. The fully-charged ratio is obviously improved with C2/C3.
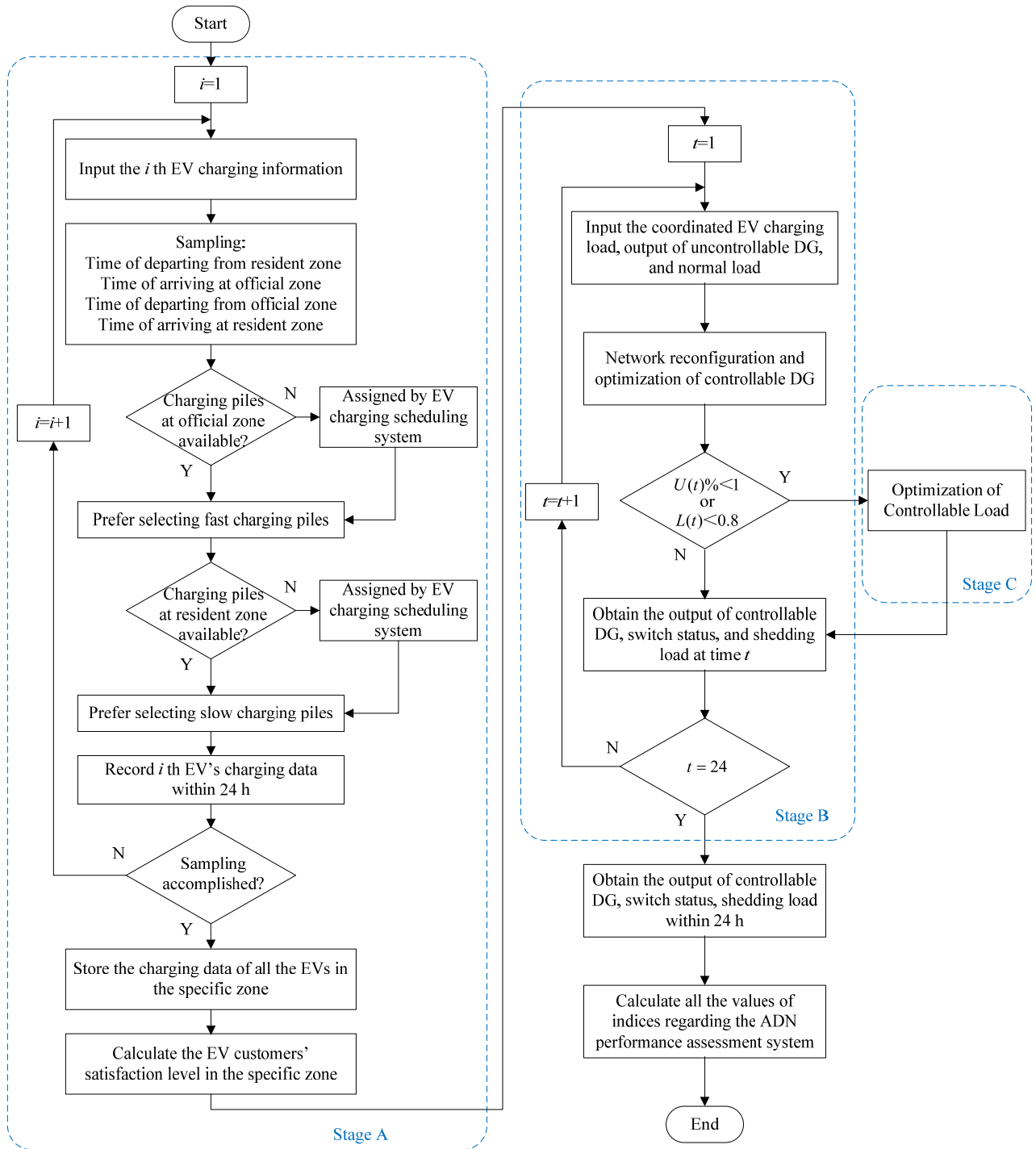
FIGURE 3. Flowchart of the multi-stage optimization approach.

In addition to the previous comparison of EV charging status with different charging modes, the impact of the coordinated EV charging mode on the daily load curve is also analyzed. As shown in Fig. 6, the peak load is significantly increased with the conventional charging mode. By contrast, the charging periods are distributed in the valley-load and flat-load intervals, which contribute to the peak-shaving and valley-filling function.

The indices regarding the assessment system for ADN performance are shown in TABLE 2. After the coordinated EV charging scheduling, the EV customers' satisfaction level is notably enhanced with lower charging cost and higher
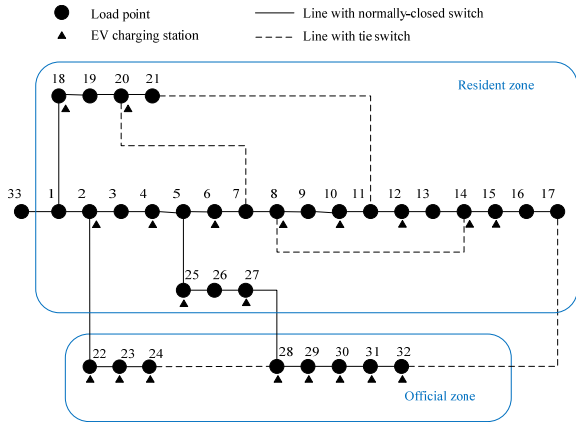
FIGURE 4. Topology of the modified IEEE 33-bus test system.

fully-charged ratio. Also, the daily load curve is more smoothing, which is consistent with the equivalent load curve standard deviation.

B. CONTROLLABLE DG AND NETWORK TOPOLOGY OPTIMIZATION

In this stage, the total load consists of the initial load and the EV load after the optimization in Stage A. Assume that three microturbines are connected to bus 12, 23, and 31, respectively. Also, #1-#32 are normal switches and #33∼#37 are tie switches, locations of the switches can be seen in Appendix. The switch status, outputs of each microturbine, and qualified voltage ratio are listed in TABLE 3, TABLE 4, and TABLE 5, respectively.

TABLE 2. Satisfaction level of EV customer and equivalent load curve standard deviation in different charging modes.

Indices		Unit	Values	
			C0	C3
Satisfaction level of EV customer	Average fully-charged ratio	%	80.7	97.7
	Average charging cost	CNY	25.08	17.32
Equivalent load curve standard deviation		kW/h	1876.16	1817.93

It can be observed that three network reconfigurations happen at time 11, 17, and 20, respectively, when the grid load surges. It indicates that reconfiguration process is likely to be implemented at these peak-load hours. In addition, the microturbines act at time 10, and 14∼21, providing a complementary support on the ADN performance. Also, except for the values of qualified voltage ratio at time 20 and 21, the others are equal to 100% after the optimization in Stage B. Besides, the relative indices in terms of the ADN performance assessment system are shown in TABLE 6. It is obviously that all the listed indices (except of the switch operation cost) are improved.

C. CONTROLLABLE LOAD OPTIMIZATION

It is worth noting that values of the qualified voltage ratio at time 20 and 21 are still less than 100% after the aforementioned two-stage optimization. Thus, the controllable load optimization is simulated in the third stage. Assume that both
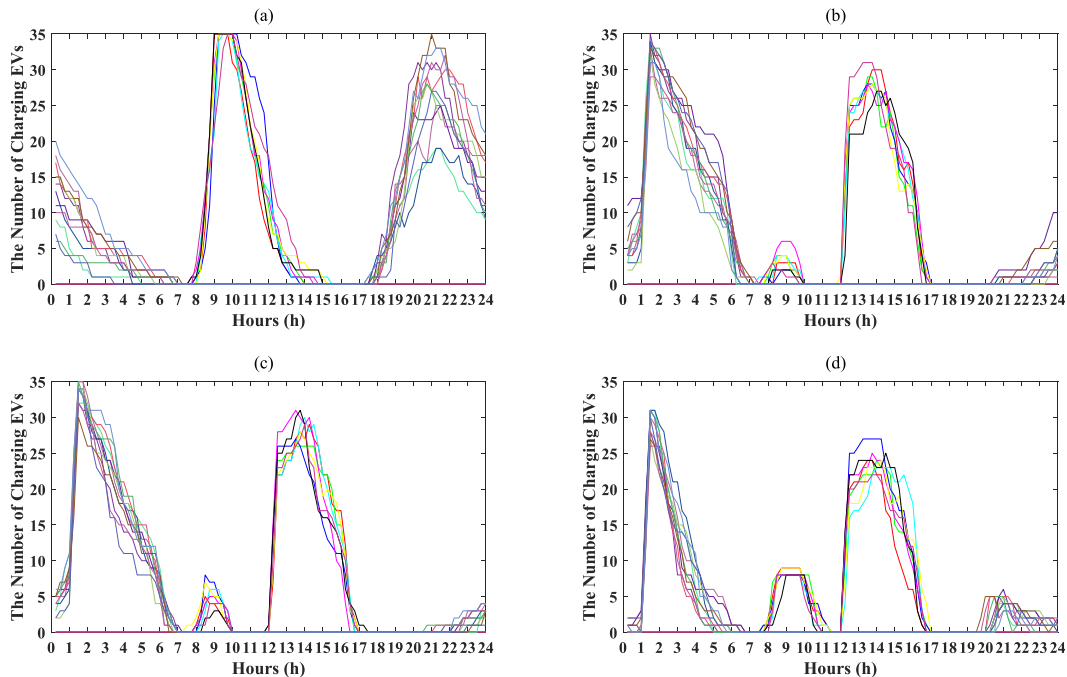

FIGURE 5. The status of EV charging stations in different charging scheduling modes. (a) C0. (b) C1. (c) C2. (d) C3.

TABLE 3. The status of switch and network reconfiguration.

Time	1	2	3	4	5	6	7	8	9	10	11	12
Switch on No.	33~37	33~37	33~37	33~37	33~37	33~37	33~37	33~37	33~37	33~37	7 14 28 35 36	7 14 28 35 36
Network Reconfigured	×	×	×	×	×	×	×	×	×	×	√	×
Time	13	14	15	16	17	18	19	20	21	22	23	24
Switch on No.	7 14 28 35 36	7 14 28 35 36	7 14 28 35 36	7 14 28 35 36	7 10 14 27 36	7 10 14 27 36	7 10 14 27 36	7 10 13 27 36	7 10 13 27 36	7 10 13 27 36	7 10 13 27 36	7 10 13 27 36
Network Reconfigured	×	×	×	×	√	×	×	√	×	×	×	×

TABLE 4. Outputs of microturbines.

Time	1	2	3	4	5	6	7	8	9	10	11	12
MT1	0	0	0	0	0	0	0	0	0	0	0	0
MT2	0	0	0	0	0	0	0	0	0	0	0	0
MT3	0	0	0	0	0	0	0	0	0	33.33	0	0
Time	13	14	15	16	17	18	19	20	21	22	23	24
MT1	0	0	0	4.76	0	0	0	300	300	0	0	0
MT2	0	0	0	171.43	61.91	4.76	300	295.23	295.23	0	0	0
MT3	0	4.76	228.57	295.24	252.38	295.24	300	300	300	0	0	0
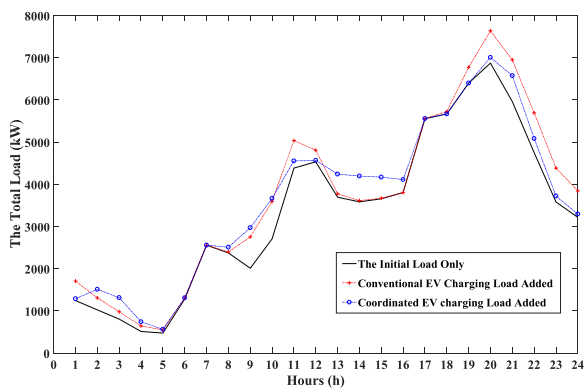
FIGURE 6. The comparison of daily load curves with different EV charging modes.

FIGURE 7. The daily load curve with EV load shedding.

the EV load and interruptible load are the controllable load sources and the load shedding process is prior to be implemented on the EV load. After temporarily shutting down all the charging piles at time 20 and 21, the total loads decrease during this period, as shown in Fig. 7. However, values of the qualified voltage ratio remain unchanged. Then, with the interruptible load shedding, this index increases from 90.91% to 100%. The shedding loads at time 20 and 21 are 269.82 kW and 440.71 kW, respectively.

D. COMPREHENSIVE EVALUATION FOR ADN PERFORMANCE

According to the proposed assessment method, the indices after the multi-stage optimal scheduling are listed in TABLE 7.

In terms of active controllability, the average qualified voltage ratio increases from 82.7% to 100% and the average primary line load ratio decreases from 41.57% to 38.32% after the initial network is reconfigured and the controllable load is dispatched. In addition, from the perspective of

TABLE 5. Qualified voltage ratio before/after stage B.

Time	1	2	3	4	5	6	7	8	9	10	11	12
U_{bef}%	100	100	100	100	100	100	100	100	100	100	81.81	81.81
U_{aft}%	100	100	100	100	100	100	100	100	100	100	100	100
Time	13	14	15	16	17	18	19	20	21	22	23	24
U_{bef}%	93.93	87.87	87.87	84.84	54.54	51.51	45.45	36.36	39.39	57.57	100	100
U_{aft}%	100	100	100	100	100	100	100	90.91	90.91	100	100	100

TABLE 6. The comparison of indices before/after stage B.

Indices	Unit	Values	
		Before Stage B	After Stage B
Average qualified voltage ratio	%	83.45	99.24
Average primary line load ratio	%	41.32	38.31
Distribution system loss cost	CNY	3156.14	2127.89
Power source integration cost	CNY	44549.34	44270.78
Environmental pollution penalty	CNY	1681.76	1615.49
Switch operation cost	CNY	0	240

active manageability, the EV customers' satisfaction level is enhanced, along with the daily load curve being smoothed with the help of coordinated EV charging strategy and overload shedding. Also, the cost regarding the active economy are significantly lowered: 1) distribution system loss cost decreased from 3309.06 CNY to 2118.66 CNY, 2) power source integration cost decreased from 44771.85 CNY to 43797.34 CNY, and 3) environmental pollution penalty decreased from 1691.43 to 1606.03 CNY.

V. CONCLUSION

In this paper, a multi-stage optimization approach for ADN scheduling considering coordinated EV charging strategy is proposed. First, an assessment system for ADN performance is established from the perspective of active controllability, active manageability, and active economy. Second, the multi-stage ADN scheduling approach integrates the optimization of coordinated EV charging scheduling, controllable DG, network topology, and controllable load, providing an adjustable dispatch scheme based on the ADN performance assessment system. Finally, the multi-stage optimization process is simulated and quantitative assessment for ADN performance is demonstrated with case studies.

From the work presented in this paper, the following conclusions can be made:

1) The coordinated EV charging strategy has a notably ameliorative impact on EV customers' satisfaction level. Meanwhile, it contributes to the function of peak shaving and valley filling, especially when intermittent sources are connected into the power grid.

2) The ADN performance assessment system is able to provide a quantitative analysis on the active controllability, active manageability, and active economy, which can serve as a comprehensive criterion of ADN scheduling.

TABLE 7. The indices regarding the assessment system for ADN performance.

AND performance	Indices		Unit	Values	
				Before	After
Active controllability	Average qualified voltage ratio		%	82.7	100
	Average primary line load ratio		%	41.57	38.32
	Switch frequency		time(s)	0	12
Active manageability	Satisfaction level of EV customer	Average fully-charged ratio	%	80.7	93.25
		Average charging cost	CNY	25.08	15
	Equivalent load curve standard deviation		kW/h	2006.24	1770.52
	Interruptible load compensation		CNY	0	980.52
Active economy	Distribution system loss cost		CNY	3309.06	2118.66
	Power source integration cost		CNY	44771.85	43797.34
	Environmental pollution penalty		CNY	1691.43	1606.03

TABLE 8. The probabilistic parameters regarding EV's charging time.

Time of departing from resident zone	$N(7,0.5^2)^*$
Time of arriving at official zone	$N(9,0.5^2)$
Time of departing from official zone	$N(18,0.5^2)$
Time of arriving at resident zone	$N(19,1.5^2)$

$^*N(7,0.5^2)$ means the expected value of the time of departing from resident zone is 7:00 and the standard deviation is 0.5 h in the typical day.

TABLE 9. The Time-of-Use (TOU) price for EV charging.

Time	Charging price (CNY/kW·h)
01:01-6:00	0.4
00:01-01:00, 6:01-10:00, 12:01-17:00, 22:01-00:00	1.2
10:01-12:00, 17:01-22:00	2

TABLE 10. Test system parameters.

Time	1	2	3	4	5	6	7	8
Resident load (kW)	584.29	438.21	292.14	146.07	146.07	1022.50	2191.07	1898.93
Commercial load (kW)	659.21	585.96	512.72	366.23	329.61	256.36	366.23	476.10
Photovoltaic (kW)	0.00	0.00	0.00	0.00	0.00	0.40	1.60	7.00
Wind power (kW)	343.43	343.43	313.13	303.03	222.22	157.58	141.41	202.02
Time	9	10	11	12	13	14	15	16
Resident load (kW)	1314.64	1241.61	2848.39	2921.43	2045.00	1387.68	1314.64	1022.50
Commercial load (kW)	695.83	1464.91	1538.16	1611.40	1648.03	2197.37	2343.86	2783.33
Photovoltaic (kW)	20.00	46.00	46.60	63.60	86.60	74.00	80.60	66.00
Wind power (kW)	147.47	121.21	80.81	40.40	137.37	165.66	121.21	86.87
Time	17	18	19	20	21	22	23	24
Resident load (kW)	2775.36	2921.43	3651.79	3943.93	3067.50	2921.43	2191.07	2118.04
Commercial load (kW)	2783.33	2746.71	2746.71	2929.82	2893.20	1831.14	1391.67	1098.68
Photovoltaic (kW)	47.60	26.60	8.60	0.60	0.00	0.00	0.00	0.00
Wind power (kW)	165.66	145.45	202.02	238.38	228.28	252.53	266.67	282.83

TABLE 11. Locations of the switches in the modified IEEE 33-Bus test system.

Switch No.		1	2	3	4	5	6	7	8	9	10	11	12	13	14	15	16	17	18	19
Bus No.	From	33	1	2	3	4	5	6	7	8	9	10	11	12	13	14	15	16	1	18
	To	1	2	3	4	5	6	7	8	9	10	11	12	13	14	15	16	17	18	19
Switch No.		20	21	22	23	24	25	26	27	28	29	30	31	32	33	34	35	36	37	-
Bus No.	From	19	20	2	22	23	5	25	26	27	28	29	30	31	7	8	11	17	24	-
	To	20	21	22	23	24	25	26	27	28	29	30	31	32	20	14	21	32	28	-

3) By cooperating with the ADN performance assessment system, the multi-stage optimization approach is able to adequately coordinate the scheduling of ADN's source-side, network-side, and demand-side.

As future work, we plan to extend the proposed EV dispatch model to incorporate the impact of participation in the V2G smart grid activities, combining with the battery degradation characteristics. Another important extension is incorporating the spatial uncertainties of the EV load demand into our framework, through establishing a probabilistic EV load model considering both the distribution of assembled EV charging piles and the electric range of EV. We also consider adding energy storage deployments in the proposed ADN framework to cooperate with other DERs.

APPENDIX
Tables 8, 9, 10, and 11.

REFERENCES

[1] J.-Y. Joo, S. Raghavan, and Z. Sun, "Integration of sustainable manufacturing systems into smart grids with high penetration of renewable energy resources," in *Proc. IEEE Green Technol. Conf. (Green Tech)*, Kansas City, MO, USA, Apr. 2016, pp. 12–17.

[2] Q. Shi, H. Hu, W. Xu, and J. Yong, "Low-order harmonic characteristics of photovoltaic inverters," *Int. Trans. Electr. Energ. Syst.*, vol. 26, no. 2, pp. 347–364, Feb. 2016.

[3] M. R. Dorostkar-Ghamsari, M. Fotuhi-Firuzabad, M. Lehtonen, and A. Safdarian, "Value of distribution network reconfiguration in presence of renewable energy resources," *IEEE Trans. Power Syst*, vol. 31, no. 3, pp. 1879–1888, May 2016.

[4] P. Gao, H. Chen, X. Zheng, and B. Wu, "Framework planning of active distribution network considering active management," *J. Eng.*, vol. 2017, no. 13, pp. 2093–2097, Nov. 2017, doi: 10.1049/joe.2017.0699.

[5] S. Pirouzi, J. Aghaei, T. Niknam, H. Farahmand, and M. Korpås, "Proactive operation of electric vehicles in harmonic polluted smart distribution networks," *IET Generat., Transmiss. Distrib.*, vol. 12, no. 4, pp. 967–975, Feb. 2018.

[6] F. Gou, J. Yang, and T. Zang, "Ordered charging strategy for electric vehicles based on load balancing," in *Proc. IEEE Conf. Energy Internet Energy Syst. Integr. (EI2)*, Beijing, China, Nov. 2017, pp. 1–5.

[7] H. Cui, F. Li, X. Fang, and R. Long, "Distribution network reconfiguration with aggregated electric vehicle charging strategy," in *Proc. IEEE Power Energy Soc. Gen. Meeting*, Denver, CO, USA, Jul. 2015, pp. 1–5.

[8] N. Wang, "The key technology of the control system of wind farm and photovoltaic power plant cluster," in *Proc. Int. Conf. Power Syst. Technol.*, Chengdu, China, Oct. 2014, pp. 2831–2839.

[9] X. Li, D. Hui, and X. Lai, "Battery energy storage station (BESS)-based smoothing control of photovoltaic (PV) and wind power generation fluctuations," *IEEE Trans. Sustain. Energy*, vol. 4, no. 2, pp. 464–473, Apr. 2013.

[10] I. I. Atteya, H. Ashour, N. Fahmi, and D. Strickland, "Radial distribution network reconfiguration for power losses reduction using a modified particle swarm optimisation," *CIRED-Open Access Proc. J.*, vol. 2017, no. 1, pp. 2505–2508, Jun. 2017, doi: 10.1049/oap-cired.2017.1286.

[11] R. Sun, H. Zhu, and Y. Liu, "A r-NSGA-II algorithm based generator start-up for network reconfiguration," in *Proc. 5th Int. Conf. Electr. Utility Deregulation Restruct. Power Technol. (DRPT)*, Changsha, China, Nov. 2015, pp. 1332–1335.

[12] C. Chen *et al.*, "Network configuration based on basic ring matrix and improved harmony search algorithm," *Autom. Electr. Power Syst.*, vol. 38, no. 6, pp. 55–60, Mar. 2014.

[13] X. Gu and H. Zhong, "Optimisation of network reconfiguration based on a two-layer unit-restarting framework for power system restoration," *IET Generation, Transmiss. Distribution*, vol. 6, no. 7, pp. 693–700, Jul. 2012.

[14] C. Zhang, Z. Lin, F. Wen, G. Ledwich, and Y. Xue, "Two-stage power network reconfiguration strategy considering node importance and restored generation capacity," *IET Generat., Transmiss. Distrib.*, vol. 8, no. 1, pp. 91–103, Jan. 2014.

[15] O. Malík and P. Havel, "Active demand-side management system to facilitate integration of RES in low-voltage distribution networks," *IEEE Trans. Sustain. Energy*, vol. 5, no. 2, pp. 673–681, Apr. 2014.

[16] Q. Shi, F. Li, Q. Hu, and Z. Wang, "Dynamic demand control for system frequency regulation: Concept review, algorithm comparison, and future vision," *Electr. Power Syst. Res.*, vol. 154, pp. 75–87, Jan. 2018.

[17] H. Xing, H. Cheng, Y. Zhang, and P. Zeng, "Active distribution network expansion planning integrating dispersed energy storage systems," *IET Generat., Transmiss. Distrib.*, vol. 10, no. 3, pp. 638–644, Mar. 2016.

[18] H. Zhang, D. Zhao, C. Gu, F. Li, and B. Wang, "Economic optimization of smart distribution networks considering real-time pricing," *J. Mod. Power Syst. Clean Energy*, vol. 2, no. 4, pp. 350–356, Dec. 2014.

[19] H. Manoochehri and A. Fereidunian, "A multimarket approach to peak-shaving in smart grid using time-of-use prices," in *Proc. 8th Int. Symp. Telecommun. (IST)*, Tehran, Iran, Sep. 2016, pp. 707–712.

[20] K. Clement-Nyns, E. Haesen, and J. Driesen, "The impact of charging plug-in hybrid electric vehicles on a residential distribution grid," *IEEE Trans. Power Syst.*, vol. 25, no. 1, pp. 371–380, Feb. 2010.

[21] J. Taylor, A. Maitra, M. Alexander, D. Brooks, and M. Duvall, "Evaluations of plug-in electric vehicle distribution system impacts," in *Proc. IEEE Power Energy Soc. Gen. Meeting*, Providence, RI, USA, Jul. 2010, pp. 1–6.

[22] C. M. Martinez, X. Hu, D. Cao, E. Velenis, B. Gao, and M. Wellers, "Energy management in plug-in hybrid electric vehicles: Recent progress and a connected vehicles perspective," *IEEE Trans. Veh. Technol.*, vol. 66, no. 6, pp. 4534–4549, Jun. 2017.

[23] X. Wu, X. Hu, S. Moura, X. Yin, and V. Pickert, "Stochastic control of smart home energy management with plug-in electric vehicle battery energy storage and photovoltaic array," *J. Power Sources*, vol. 333, pp. 203–212, Nov. 2016.

[24] X. Wu, X. Hu, Y. Teng, S. Qian, and R. Cheng, "Optimal integration of a hybrid solar-battery power source into smart home nanogrid with plug-in electric vehicle," *J. Power Sources*, vol. 363, pp. 277–283, Sep. 2017.

[25] D. Yu *et al.*, "Synergistic dispatch of PEVs charging and wind power in Chinese regional power grids," *Autom. Electr. Power Syst.*, vol. 35, no. 14, pp. 24–29, Jul. 2011.

[26] T. K. Kristoffersen, K. Capion, and P. Meibom, "Optimal charging of electric drive vehicles in a market environment," *Appl. Energy*, vol. 88, pp. 1940–1948, May 2011.

[27] M. Kintner-Meyer, K. Schneider, and R. Pratt, "Impacts assessment of plug-in hybrid vehicles on electric utilities and regional U.S. power grids part 1: Technical analysis," Pacific Northwest Nat. Lab., Washington, DC, USA, Tech. Rep. 1, Jan. 2007, pp. 1–19.

[28] D. Wu, D. C. Aliprantis, and K. Gkritza, "Electric energy and power consumption by light-duty plug-in electric vehicles," *IEEE Trans. Power Syst.*, vol. 26, no. 2, pp. 738–746, May 2011.

[29] S. Bae and A. Kwasinski, "Spatial and temporal model of electric vehicle charging demand," *IEEE Trans. Smart Grid*, vol. 3, no. 1, pp. 394–403, Mar. 2012.

[30] C. Zhang, J. Jiang, Y. Gao, W. Zhang, Q. Liu, and X. Hu, "Charging optimization in lithium-ion batteries based on temperature rise and charge time," *Appl. Energy*, vol. 194, pp. 569–577, May 2017.

[31] C. Zou, X. Hu, Z. Wei, and X. Tang, "Electrothermal dynamics-conscious lithium-ion battery cell-level charging management via state-monitored predictive control," *Energy*, vol. 141, pp. 250–259, Dec. 2017.

[32] K. Qian, C. Zhou, M. Allan, and Y. Yuan, "Modeling of load demand due to EV battery charging in distribution systems," *IEEE Trans. Power Syst.*, vol. 26, no. 2, pp. 802–810, May 2011.

[33] M. Sedghi, A. Ahmadian, and M. Aliakbar-Golkar, "Optimal storage planning in active distribution network considering uncertainty of wind power distributed generation," *IEEE Trans. Power Syst.*, vol. 31, no. 1, pp. 304–316, Jan. 2016.

[34] A. Ahmadian, M. Sedghi, M. Aliakbar-Golkar, A. Elkamel, and M. Fowler, "Optimal probabilistic based storage planning in tap-changer equipped distribution network including PEVs, capacitor banks and WDGs: A case study for Iran," *Energy*, vol. 112, pp. 984–997, Oct. 2016.

[35] A. Ahmadian, M. Sedghi, A. Elkamel, M. Aliakbar-Golkar, and M. Fowler, "Optimal WDG planning in active distribution networks based on possibilistic–probabilistic PEVs load modelling," *IET Generat., Transmiss. Distrib.*, vol. 11, no. 4, pp. 865–875, Mar. 2017.

[36] A. Ahmadian, M. Sedghi, A. Elkamel, M. Fowler, and MA. Golkar, "Plug-in electric vehicle batteries degradation modeling for smart grid studies: Review, assessmentand conceptual framework," *IET Generat., Transmiss. Distrib.*, vol. 11, no. 4, pp. 865–875, Mar. 2017.

[37] A. Ahmadian, M. Sedghi, B. Mohammadi-Ivatloo, A. Elkamel, M. A. Golkar, and M. Fowler, "Cost-Benefit analysis of V2G implementation in distribution networks considering PEVs battery degradation," *IEEE Trans. Sustain. Energy*, vol. 9, no. 2, pp. 961–970, Apr. 2018.

XIAOJUN ZHU received the B.S. degree from the Nanjing University of Aeronautics and Astronautics, China, in 2013, and the M.S. degree from Southeast University, China, in 2016. She is currently an Engineer with the State Grid Jiangsu Economic Research Institute. Her research interests include distribution network planning, energy storage deployment, and transformer substation designing.
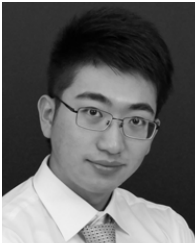
HAITENG HAN (S'15) received the B.S. degree from Southeast University, China, in 2010, where he is currently pursuing the Ph.D. degree. His research interests include power system computing, demand response, security assessment, and power system operation and control.
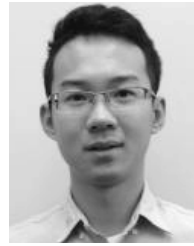
HANTAO CUI (S'13) received the B.S. and M.S. degrees from Southeast University, China, in 2011 and 2013, respectively, and the Ph.D. degree from The University of Tennessee, Knoxville, TN, USA, in 2018. He is currently a Research Associate with the Center for Ultra-wide-area Resilient Electric Energy Transmission Networks. His research interests include energy storage systems, demand response, and large-scale power system simulations.

SHAN GAO (M'11) received the B.S. degree from Shandong University, China, in 1994, and the M.S. and Ph.D. degrees from Southeast University, China, in 1997 and 2000, respectively. He is currently an Associate Professor at Southeast University. His research interests include power system operation, smart dispatching, and active distribution networks.

QINGXIN SHI (S'11) received the B.S. degree from Zhejiang University, China, in 2011, and the M.S. degree from the University of Alberta, Canada, in 2014. He is currently pursuing the Ph.D. degree with The University of Tennessee, Knoxville, TN, USA. His research interests include demand response and dynamic demand control for system frequency regulation.

GUOQIANG ZU (S'15) received the B.S. and Ph.D. degrees from Tianjin University in 2012 and 2017, respectively. He is currently an Engineer with the State Grid Tianjin Electric Power Company Electric Power Research Institute. His research interests include planning, assessment, and operation of smart distribution grids, distributed energy resources, and urban energy Internet.

• • •